# FRICTION IDENTIFICATION BASED UPON THE LUGRE AND MAXWELL SLIP MODELS ⋆

**Demosthenis D. Rizos** *and* **Spilios D. Fassois** [1]

*Stochastic Mechanical Systems (SMS) Group*
*Department of Mechanical & Aeronautical Engineering*
*University of Patras, GR 265 00 Patras, Greece*
*E-mail: {driz,fassois}@mech.upatras.gr*
*Internet: http://www.mech.upatras.gr/∼sms*

Abstract: Three friction identification methods, designated as the LuGre (LG) method, the Non-Linear Regression (NLR) method, and the Dynamic Non-Linear Regression with direct application of the eXcitation (DNLRX) method, are postulated. The first employs the LuGre model structure, the second the basic Maxwell Slip model structure, and the third an extended version of it. The Maxwell Slip model structure accounts for the presliding hysteresis with nonlocal memory, but is confined to providing constant sliding friction. This limitation is circumvented by the extended version postulated, where additional dynamics are introduced. In all methods identification is based upon signals obtained from a single experiment, thus circumventing the need for multiple experiments. The methods are assessed via laboratory signals, and the DNLRX is shown to achieve the best overall performance, followed by the NLR and, finally, the LG method. 

Keywords: Friction, identification.

## 1. INTRODUCTION

Friction is a major nonlinear phenomenon that may lead to tracking errors, limit cycles, stick and slip motion, and so on. Its behavior may be distinguished into two operating regimes: The *presliding (micro-slip)* and the *sliding* regimes. In the first the adhesive forces are dominant, and friction depends, among other factors, on the past extreme values of the displacement, thus exhibiting hysteresis within nonlocal memory (Swevers *et al.*, 2000). This hysteresis disappears upon switching from the *presliding* to the *sliding* regime. Within the latter regime friction depends mainly on the velocity, and various nonlinear phenomena (such as the *Stribeck effect, frictional lag* and so on) are exhibited (Armstrong-Hélouvry *et al.*, 1994).

Accurate friction modelling based upon the first principles and material / surface properties is not possible to date. Thus, identification methods based upon experimentally obtained signals are typically used. Classical methods relate friction directly to velocity and / or displacement, and attempt identification via either time domain (Armstrong-Hélouvry *et al.*, 1994; Kim *et al.*, 1996) or frequency domain techniques (Chen *et al.*, 2002). The obtained models generally tend to oversimplify the actual frictional behavior.

More elaborate methods relate friction to velocity and/or displacement via internal (unobservable) *state variables*. The underlying dynamics is better described, but the identification becomes more challenging. In general, identification is achieved by separating the unknown parameters into *static* and *dynamic*, corresponding to the sliding and presliding regimes, respectively, and performing dedicated experiments in each regime. A notable class of such methods relies on the LuGre model (Canudas de Wit and Lischin-

⋆ Research supported by the VolkswagenStiftung – Grant no I/76938.
[1] Corresponding author. Tel/Fax: ++30 2610 997 405, Email: `fassois@mech.upatras.gr`

sky, 1997; Hensen *et al.*, 2002) and its extension, referred to as the Elastoplastic friction model (Dupont *et al.*, 2002). An alternative method is based upon the Leuven friction model (Swevers *et al.*, 2000), which is similar to the LuGre model, but extended for capturing the presliding hysteresis with nonlocal memory.

The current study *aims* at identifying the combined presliding / sliding friction dynamics based upon the LuGre and Maxwell Slip model structures. Three identification methods, designated as the LG method (LuGre), the NLR (NonLinear Regression) method, and the DNLRX (Dynamic NonLinear Regression with direct application of the eXitation) method, are formulated and assessed. The first employs the LuGre model structure. The second employs the basic Maxwell Slip model structure, and is thus capable of accounting for the presliding hysteresis with nonlocal memory (Lampaert *et al.*, 2002), but may only provide constant sliding friction. The third circumvents this limitation by employing a presently formulated extended form of the Maxwell Slip model structure that makes use of two finite impulse response filters.

In all methods identification is based upon a single pair of displacement – friction signals. The experimental procedure is thus simplified, as the usual need for several dedicated experiments is circumvented.

## 2. MODEL STRUCTURES

### 2.1 *The LuGre Model Structure*

The LuGre model structure (Canudas de Wit *et al.*, 1995) contains an unobservable state variable $z$, representing the average deflection of the elastic "bristles" that are responsible for friction generation. It accounts for most of the observed frictional dynamics, but the presliding hysteresis with nonlocal memory is not represented (Swevers *et al.*, 2000).

The LuGre model features the nonlinear state equation:

$$\frac{dz}{dt} = v - \frac{|v|}{s(v)} \cdot z \qquad (1)$$

and an output equation for approximating the frictional force as follows:

$$F_{LG} = \sigma_0 \cdot z + \sigma_1 \cdot \frac{dz}{dt} + \sigma_2 \cdot v \qquad (2)$$

with $v$ designating velocity, $\sigma_0$ an equivalent stiffness, and $\sigma_1$, $\sigma_2$ the micro-viscous and viscous friction coefficients, respectively. $s(v)$ designates a user-defined function that models the constant-velocity behavior. The following parametrization, similar to a typical one (Armstrong-Hélouvry *et al.*, 1994), is presently adopted for $s(v)$:

$$s(v) = a_1 + \frac{a_2}{1 + \left(\frac{|v|}{v_s}\right)^{\mu}}, \; a_1 = \frac{F_c}{\sigma_0}, \; a_2 = \frac{F_s - F_c}{\sigma_0} \qquad (3)$$

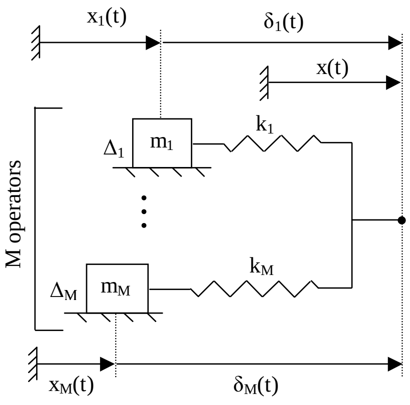


Fig. 1. The basic Maxwell Slip model structure.

with $F_c$ and $F_s$ designating the *Coulomb* and *static* friction, respectively, $v_s$ the *Stribeck* velocity, and $\mu$ a parameter providing for extra modelling flexibility.

### 2.2 *Structures Based Upon the Maxwell Slip Model*

*The Basic Structure.* The basic Maxwell Slip model structure consists of $M$ elasto-slide operators in parallel configuration, which are subject to a common displacement excitation $x(t)$ [Fig. 1]. Each operator has negligible inertia, its own linear stiffness $k_i$, and maximum spring deformation $\Delta_i$ (threshold). For spring deformation smaller, in magnitude, than $\Delta_i$ ($|\delta_i(t)| < \Delta_i$) the operator *sticks*; otherwise it *slips* ($|\delta_i(t)| = \Delta_i$). The whole system sticks (presliding regime) iff at least one operator sticks ($\exists j \in [1, M]$ : $|\delta_j(t)| < \Delta_j$), and slides (sliding regime) iff all operators slip ($|\delta_i(t)| = \Delta_i, \forall i$).

In mathematical terms, the model is described by a set of nonlinear state equations (Rizos and Fassois, 2004):

$$\delta_i(t+1) = \text{sgn}[x(t+1) - x(t) + \delta_i(t)] \cdot \\ \cdot \min\{|x(t+1) - x(t) + \delta_i(t)|, \Delta_i\} \qquad (4)$$

with $i = 1, \ldots, M$, while the friction is approximated as the sum of the operators' forces:

$$F_M(t) = \sum_{i=1}^{M} k_i \cdot \delta_i(t) \qquad (5)$$

with $t = 1, 2, \ldots$ referring to (normalized) discrete time.

Among the main advantages of this basic structure is simplicity, physical interpretation, and its capability of describing the presliding hysteresis with nonlocal memory (Lampaert *et al.*, 2002). Yet, the model accounts for constant sliding (Coulomb) friction only [see Eq. (5) and recall that the system slides iff $|\delta_i(t)| = \Delta_i, \forall i$, that is iff *all* operators slip]. It is evident that this constraint may impair modelling accuracy, hence a proper extension is introduced in the sequel.

*The Extended Structure.* The extension is based upon a suitable modification of the linear part [Eq. (5)] of the basic structure. The frictional force is now allowed to depend upon *present* and *past* values of the spring deformations [$\delta_i(t)$'s], as well as upon values of the displacement itself. This is accomplished by having the displacement driven through a Finite Impulse Response (FIR) filter of order $n_x$ [with coefficients $c_r$ ($r = 0, \ldots, n_x$)] and the spring deformation vector $\boldsymbol{\delta}(t)$ (note that bold face lower/upper case symbols designate vector/matrix quantities, respectively), defined as:

$$\boldsymbol{\delta}(t) \triangleq [\delta_1(t) \ldots \delta_M(t)]^T ,$$

through an $M$-dimensional FIR filter of order $n$ [with vector coefficients $\boldsymbol{\theta}_r$ ($r = 0, \ldots, n$)]. The extended structure thus is of the form:

$$F_{EM}(t) = \sum_{r=0}^{n_x} c_r \cdot x(t-r) + \sum_{r=0}^{n} \boldsymbol{\theta}_r^T \cdot \boldsymbol{\delta}(t-r) \quad (6)$$

subject to Eq. (4). The first part of Eq. (6) allows for friction dependency upon the displacement history. Since velocity may be obtained via numerical differentiation of displacement, this part may be considered as a discrete - time equivalent of the friction dependency upon velocity and may account for the *viscous* friction, as well as for *frictional lag*.

The second part provides for the friction dependence upon the current and past values of the spring deformations, and this may be also considered as a discrete - time analogue of the existence of a micro - viscous effect.

The extended structure retains the simplicity of its basic counterpart, in the sense that the nonlinear part of the model [Eq. (4)] remains unchanged. It also features additional dynamics and flexibility owing to the introduced Finite Impulse Response (FIR) filters. This may (to a certain extent) account for discrepancies between the basic structure and the actual friction dynamics. The price paid for this is that extra parameters are introduced.

## 3. FRICTION IDENTIFICATION METHODS

The postulated identification methods are based upon the previously mentioned model structures. The *LG method* utilizes the LuGre model structure and is mainly presented for purposes of comparison. The *NonLinear Regression (NLR) method* employs the basic Maxwell Slip structure and has been previously applied to pure *presliding* friction identification (Rizos and Fassois, 2004). The *Dynamic NonLinear Regression with direct application of the eXcitation (DNLRX) method* employs the extended model structure presented in the previous section.

All methods attempt identification based upon a single pair of displacement (excitation) – friction (response) signals, thus circumventing the usual need for a series of dedicated experiments. This is done by minimizing a quadratic cost function of the form:

$$\mathcal{J} \triangleq \sum_{t=\lambda}^{N} e^2(t) \quad (7)$$

with $N$ designating the length of the available signals, while $\lambda \equiv 1$ for the LG and NLR methods and $\lambda \equiv \max\{n, n_x\} + 1$ for the DNLRX method. $e(t)$ is the error defined as the difference between the measured, $F(t)$, and the model provided, $\bar{F}(t)$, friction:

$$e(t) \triangleq F(t) - \bar{F}(t) \quad (8)$$

As is conventionally done, this error is assumed to be a stationary *zero mean* and *white* sequence with variance $\sigma_e^2$ (relaxation of these assumptions is possible, but is beyond the scope of the present study).

### 3.1 *The LG Identification Method*

The LG($\boldsymbol{g}$,$\boldsymbol{\theta}_{LG}$) model is of the form [see Eq. (2)]:

$$\text{LG}(\boldsymbol{g}, \boldsymbol{\theta}_{LG})\text{: } F(t) = \boldsymbol{\theta}_{LG}^T \cdot \left[ z(t) \vdots \frac{dz(t)}{dt} \vdots v(t) \vdots 1 \right]^T + e(t) \quad (9)$$

subject to Eqs. (1) and (3). The vectors $\boldsymbol{g}$ and $\boldsymbol{\theta}_{LG}$ incorporate the model parameters:

$$\boldsymbol{g} \triangleq [z(0)\, a_1\, a_2\, v_s\, \mu]^T , \quad \boldsymbol{\theta}_{LG} \triangleq [\sigma_0\, \sigma_1\, \sigma_2\, b]^T \quad (10)$$

where $z(0)$ designates the initial value of the unmeasurable state variable $z(t)$, and $b$ an extra parameter for compensating for the experimental friction offset that may appear due to potential sensor bias.

Obviously, the model is nonlinear with respect to $\boldsymbol{g}$ [Eqs. (1) and (3)], hence the minimization of the cost function $\mathcal{J}$ leads to a nonlinear regression type estimator. Yet, the model remains linear with respect to $\boldsymbol{\theta}_{LG}$ [Eq. (9)]. Thus, the complete estimator may be realized via a succession of nonlinear and linear regression operations (see subsection 3.3 in the sequel).

Remark: The $z(t)$ evolution may be obtained by either integrating numerically the nonlinear differential equation [Eq. (1)], or applying a proper discretization. The former procedure is presently adopted.

### 3.2 *Maxwell Slip Based Identification Methods*

*The NLR Method.* The NLR($M$) model is of the form [compare to Eq. (5)]:

$$\text{NLR}(M; \boldsymbol{d}, \boldsymbol{\theta}_M)\text{: } F(t) = \boldsymbol{\theta}_M^T \cdot \left[ \boldsymbol{\delta}^T(t) \vdots 1 \right]^T + e(t) \quad (11)$$

subject to Eq. (4), with $\boldsymbol{\theta}_M$ and the threshold vector $\boldsymbol{d}$ being defined as follows:

$$\boldsymbol{d} \triangleq [\Delta_1 \ldots \Delta_M]^T , \quad \boldsymbol{\theta}_M \triangleq [k_1 \ldots k_M\ b]^T \quad (12)$$

Like before, $b$ is an extra parameter accounting for potential sensor bias. Due to the nonlinear part of the model [Eq. (4)], minimization of the cost function $\mathcal{J}$ leads to a nonlinear regression procedure. Since the model is nonlinear only with respect to $\boldsymbol{d}$, while remaining linear with respect to $\boldsymbol{\theta}_M$, estimation may be achieved similarly to the previous case.

*The DNLRX Method.* The model is of form [see Eq. (6)]:

$$\text{DNLRX}(M, n, n_x; \boldsymbol{d}, \boldsymbol{\theta}_{EM}) : F(t) = \boldsymbol{\theta}_{EM}^T \cdot$$

$$\left[x(t) \dots x(t-n_x) \vdots \boldsymbol{\delta}^T(t) \ \dots \ \boldsymbol{\delta}^T(t-n) \vdots 1\right]^T + e(t) \tag{13}$$

subject to Eq. (4), with $\boldsymbol{\theta}_{EM}$ being the $[(n+1)\cdot M + n_x + 2]$ – dimensional composite parameter vector:

$$\boldsymbol{\theta}_{EM} \triangleq \left[c_0 \dots c_{n_x} \vdots \boldsymbol{\theta}_0^T \dots \boldsymbol{\theta}_n^T \vdots b\right]^T \tag{14}$$

Since the model is nonlinear in $\boldsymbol{d}$ and linear in $\boldsymbol{\theta}_{EM}$, model estimation may be accomplished as before.

*Initial Spring Deformations.* In order to get the cost function $\mathcal{J}$ calculated, the initial spring deformation vector $\boldsymbol{\delta}(0)$ is required. As this is not available, the following procedure may be adopted [also see (Rizos and Fassois, 2004)]. Since both the presliding and sliding regimes are considered, the system should slide when the displacement $x(t)$ attains (at time, say, $t_{cr}$) a "dominant" extreme. Thus, at time $t_{cr}$, all operators slip in the same direction with $x(t_{cr})$. If the data corresponding to $t \geq t_{cr}$ are used for identification, then the initial deformations are known $[\delta_i(0) = \text{sgn}[x(t_{cr})] \cdot \Delta_i \ (\forall i)]$.

*NLR / DNLRX Order Selection.* Since the main objective of friction identification is simulation and control, model selection is tailored to these needs and is primarily judged in terms of the identified model's simulation ability. This is evaluated via a normalized quadratic function of the model error and is referred to as the *Normalized Output Error (NOE)*:

$$NOE = \frac{\sum_{t=\lambda}^{N} \left(F(t) - \bar{F}(t)\right)^2}{\sum_{t=\lambda}^{N} \left(F(t) - m_F\right)^2} \times 100\% \tag{15}$$

where $m_F$ is the sample mean of the actual friction signal and $\lambda$ is defined in Eq. (7).

NLR($M$) model order selection (selecting the number $M$ of superimposed operators) is based upon the successive estimation of models for increasing $M$ and evaluation of the error criterion. On the other hand, DNLRX($M, n, n_x$) model order selection is based upon the estimation of models for various values of $n$ and $n_x$ for any given $M$. The final model is selected following consideration of various values of $M$. Model validation relies upon the model's simulation performance within a subset of the data, referred to as the *validation set*, that has not been used in estimation *(cross validation principle)*.

### 3.3 *Parameter Estimation*

In all methods, minimization of the cost function $\mathcal{J}$ [Eq. (7)] leads to a nonlinear regression type estimator. Moreover, all models are nonlinear with respect to certain of their parameters, generally designated as $\boldsymbol{\theta}_{nl}$, while remaining linear with respect to the rest, designated as $\boldsymbol{\theta}_l$. Hence, the estimator may be realized via a succession of nonlinear and linear regression operations (the hat designates estimator / estimate):

$$\begin{aligned}\left[\hat{\boldsymbol{\theta}}_{nl}^T \ \hat{\boldsymbol{\theta}}_l^T\right]^T &= \arg \min_{\boldsymbol{\theta}_{nl}, \boldsymbol{\theta}_l} \mathcal{J}(\boldsymbol{\theta}_{nl}, \boldsymbol{\theta}_l) \\ &= \arg \min_{\boldsymbol{\theta}_{nl}} \left\{ \min_{\boldsymbol{\theta}_l} \mathcal{J}(\boldsymbol{\theta}_l / \boldsymbol{\theta}_{nl}) \right\}\end{aligned} \tag{16}$$

in which $\boldsymbol{\theta}_{nl}$ and $\boldsymbol{\theta}_l$ are defined according to the particular method (for instance $\boldsymbol{\theta}_{nl} \equiv \boldsymbol{d}$ and $\boldsymbol{\theta}_l \equiv \boldsymbol{\theta}_M$ for the NLR method).

The nonlinear regression operation is based upon a postulated two-phase hybrid optimization scheme. The first (*pre-optimization*) phase utilizes Genetic Algorithm (GA) based optimization (Nelles, 2001, p. 126) in order to explore large areas of the parameter space and locate regions where global or local minima may exist. The second (*fine optimization*) phase utilizes the Nelder-Mead Downhill Simplex algorithm (Nelles, 2001, p. 86) for locating the exact global or local minima within the previously obtained regions.

This two-phase scheme has been shown (Rizos and Fassois, 2004) to be effective in locating the true global minimum of the cost function and circumventing problems associated with local minima, which are quite severe especially for the NLR and DNLRX methods. Furthermore, the Nelder-Mead algorithm utilizes only cost function evaluations but *no* derivative evaluations, which are not defined everywhere as the cost function is *nonsmooth* in certain areas of the parameter space (NLR and DNLRX methods).

## 4. FRICTION IDENTIFICATION RESULTS

The results are based upon data obtained from a laboratory device (Lampaert *et al.*, 2004) and have been provided by the Katholieke Universiteit Leuven (Belgium). The exerted displacement is wideband random, and the signals are sampled at $f_s = 2.5 \ kHz$. The available displacement – friction force signals are divided into three disjoint sets: A $10,000$ sample–long *estimation set* exclusively used for parameter estimation, a $34,933$ sample–long *validation set* used for model validation, and a $35,170$ sample–long *test set* used for independent evaluation and assessment of the estimated models. Note that the displacement obtains a "dominant" local extreme at time $t_{cr} = 45,068$. Thus, the *estimation set* is selected to start at that time instant.

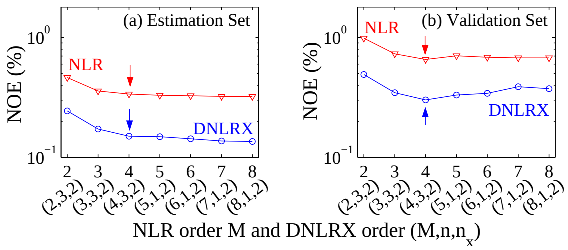


Fig. 2. NOE criterion versus model order: (a) Estimation set; (b) validation set (NLR and DNLRX models).

The *pre-optimization* phase requires the setting of bounds on the elements of vectors $\boldsymbol{d}$ [LR and DNLRX methods - Eq. (12)] and $\boldsymbol{g}$ [LG method - Eq. (10)], respectively. For the NLR and DNLRX methods bound selection is done following the guidelines prescribed in Rizos and Fassois (2004). For the LG method the bounds on $z(0)$ are set considering that at time $t_{cr}$ (the instant that the *estimation set* begins) the system slides, then, from a physical point of view, the initial average bristle deflection $z(0)$ has the same sign with $x(t_{cr})$ and cannot exceed, in amplitude, $|x(t_{cr})|$. $a_1$ and $a_2$ are positive [since $F_c, \sigma_0 > 0$ and in general $F_s - F_c \geq 0$ – Eq. (3)]. However, their upper bounds are arbitrary selected, since without performing dedicated experiments (Canudas de Wit and Lischinsky, 1997) no a priori information for $\sigma_0$, $F_c$ and $F_s$ is available. $v_s$ is by definition positive. Moreover, since it provides information regarding the velocity at which the system enters the sliding regime, its value is small compared to the maximum absolute velocity achieved during operation (Armstrong-Hélouvry *et al.*, 1994). The $\mu$ bounds may be selected as $\mu \in (0, 5]$. Note that in general $\mu = 2$ is considered (Armstrong-Hélouvry *et al.*, 1994).

### 4.1 *The LG Method*

The LG method requires the velocity signal [Eqs. (1) - (3)], which is unavailable. Thus, before applying the LG method, the velocity is estimated by first-order differencing a low-pass filtered (cut-off frequency $f_c = 0.4\ kHz$) version of the displacement signal (Dupont *et al.*, 2002).

### 4.2 *The NLR and DNLRX Methods*

The order selection procedure for the NLR method is shown in Fig. 2, which depicts the NOE criterion as a function of the number of operators included in the model. Within the *estimation set*, the NOE decreases as the order increases [Fig. 2(a)]. However, negative stiffness estimates are reported for $M \geq 5$; therefore the NLR(4) model is selected. Negative stiffness estimates should be due to the model's attempt to account for extra friction dynamics, that the model is not actually prepared to cope with (recall that this model provides only constant sliding friction). This effect is

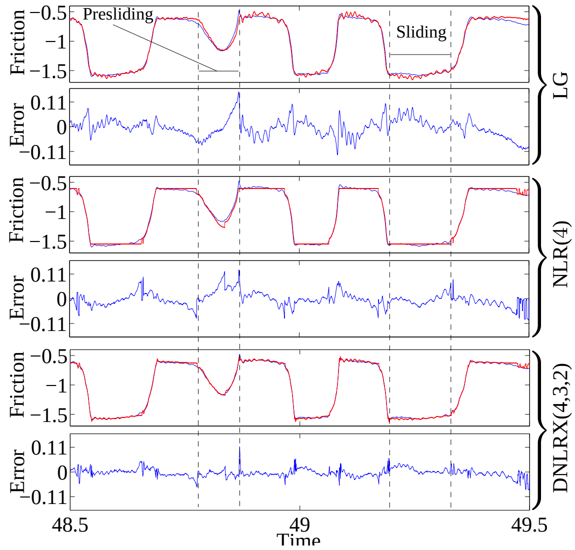


Fig. 3. Model based friction simulation (thick line) contrasted to the actual friction (slim line), and the corresponding error for each estimated model [part of the *test set*; vertical dashed lines indicate presliding / sliding regime transitions].

clearly demonstrated within the *validation set* [Fig. 2(b) – the NOE gets increased for $M > 4$].

Concerning the DNLRX method, Fig. 2 presents the FIR orders $n$ and $n_x$ (for each $M$) beyond which the NOE decrease is practically insignificant. Notice that the FIR order $n_x = 2$ is selected for all examined DNLRX models. As before, the NOE criterion within the *estimation set*, is a decreasing function of the order [Fig. 2(a)]. However, the NOE is decreasing for $M \leq 4$, remains almost unchanged for $M = 5$, and continues its decrease for $M > 5$. Thus the DNLRX$(4, 3, 2)$ is selected. This model is confirmed as a valid representation of the friction dynamics via examination of its behavior within the *validation set* [Fig. 2(b)], within which the DNLRX$(4, 3, 2)$ model achieves the globally minimum NOE.

### 4.3 *Model Performance Assessment and Comparisons*

The assessment of the obtained models is based upon their ability to simulate the measured friction. Therefore, the comparisons are in terms of the achieved NOE and MAX (model error absolute maximum) values. Additionally, the *parametric complexity* (number of estimated parameters) is also provided.

All selected models capture, though at different degrees, the underlying friction dynamics. This is confirmed by the results presented in Fig. 3, in which the measured friction is compared to the friction obtained by driving each one of the estimated models by the measured excitation (part of the *test set* is shown). The corresponding model error signal is, for each model case, also presented. A closer observation of these results (Fig. 3) reveals that the LG and NLR(4) models provide very good friction simulation within the

Table 1. Characteristics of the estimated models (test set).

| Model | LG | NLR(4) | DNLRX(4, 3, 2) |
|---|---|---|---|
| NOE$^a$ (%) | 0.67 | 0.42 | 0.24 |
| MAX$^a$ | 0.22 | 0.17 | 0.15 |
| Parametric complexity | 9 | 9 | 24 |

$^a$Simulation starting at $t_{cr} = 45,068$.

presliding regime, while excellent fit is reported by the DNLRX$(4,3,2)$ model. Regarding the sliding regime, the LG model gives, in general terms, good simulation. The NLR$(4)$ successfully predicts the regime transitions (presliding to sliding and opposite), but provides constant sliding friction. This is overcome by the DNLRX$(4,3,2)$ model, which achieves almost excellent fit within the sliding regime.

A comparative performance assessment of the three models within the *test set* is presented in Table 1. As it may be readily observed, the DNLRX$(4,3,2)$ model achieves a NOE value which is $43\%$ and $64\%$ less (approximately) than that of the NLR$(4)$ and LG models, respectively, combined with the overall best MAX value. This indicates that the proposed extension of the Maxwell Slip model structure, although incapable of reproducing the constant velocity friction characteristics like the LuGre model does [see Eq. (3)], provides extra flexibility, which significantly improves its overall performance. The price to be paid for this benefit is increased complexity (more parameters to be estimated – see Table 1). Nevertheless, this may not be necessarily a concern as the additional parameters enter the model in a linear fashion.

## 5. CONCLUSIONS

The problem of friction identification was addressed and three identification methods, referred to as LG, NLR and DNLRX, were postulated. The former is based upon the LuGre model, while the second employs the basic Maxwell Slip structure. A novel extended form of this was introduced within the third method. This extended structure combines the advantages of its basic counterpart, that is simplicity and capability of accounting for the presliding hysteresis, with the extra flexibility of two FIR filters. In all methods the model parameters are simultaneously estimated based upon a single experiment, thus overcoming the usual need for multiple dedicated experiments.

The main conclusions may be summarized as follows:

- $(i)$ The proposed methods appear capable of capturing, though at different degrees, the actual friction dynamics.
- $(ii)$ The best overall performance was unambiguously attained by the DNLRX model (with NLR scoring second and the LG third), indicating the effectiveness of the introduced extended form of the Maxwell Slip model structure.

**Acknowledgements**

The authors wish to acknowledge the financial support of this study by the VolkswagenStiftung (Grant no I/76938). Special thanks are due to the Katholieke Universiteit Leuven (KUL) research team, led by Professors H. Van Brussel and F. Al-Bender, for providing the experimental friction data, guidance, and motivation. Also to all project partners for useful discussions and fruitful collaboration.

## 6. REFERENCES

Armstrong-Hélouvry, B., P. Dupond and C. Canudas De Wit (1994). A survey of models analysis tools and compensation methods for the control of machines with friction. *Automatica* **30**, 1083 – 1138.

Canudas de Wit, C. and P. Lischinsky (1997). Adaptive friction compesation with partially known dynamic friction model. *Int. J. of Adaptive Control and Signal Processing* **11**, 65 – 80.

Canudas de Wit, C., H. Olsson, K.J. Åström and P. Lischinsky (1995). A new model for control of system with friction. *IEEE Trans. on Autom. Control* **40**, 419 – 425.

Chen, Y.-Y., P.-Y. Huang and J.-Y. Yen (2002). Frequency-domain identification algorithms for servo systems with friction. *IEEE Trans. on Control System Technology* **10**, 654 – 665.

Dupont, P., V. Hayward, B. Armstrong and F. Altpeter (2002). Single state elastoplastic friction models. *IEEE Trans. on Autom. Control* **47**, 787 – 792.

Hensen, R., M. Molengraft and M. Steinbuch (2002). Frequency domain identification of dynamic friction model parameters. *IEEE Trans. Control Syst. Technol.* **10**, 191 – 196.

Kim, J.H., H.K. Chae, J.Y. Jeon and S.W. Lee (1996). Identification and control of systems with friction using accelerated evolutionary programming. *IEEE Control Syst. Mag.* **16**, 38 – 47.

Lampaert, V., F. Al-Bender and J. Swevers (2004). Experimental chacterization of dry friction at low velocities on a developed tribometer setup for macroscopic measurements. *Tribol. Lett.* **16**, 95 – 105.

Lampaert, V., J. Swevers and F. Al-Bender (2002). Modification of the Leuven intergrated friction model structure. *IEEE Trans. on Autom. Control* **47**, 683 – 687.

Nelles, O. (2001). *Nonlinear System Identification, From Classical Approaches to Neural Networks and Fuzzy Models*. Springer-Verlag. Berlin.

Rizos, D.D. and S.D. Fassois (2004). Presliding friction identification based upon the Maxwell slip model structure. *Chaos: An Interdisciplinary Journal of Nonlinear Science* **14**, 431 – 445.

Swevers, J., F. Al-Bender, C.G. Ganseman and T. Prajogo (2000). An intergated friction model structure with improved presliding behavior for accurate friction compensation. *IEEE Trans. on Automatic Control* **45**, 675 – 686.